



EFFECT OF A SUSPENSION SYSTEM ON THE DESIGN PARAMETERS OF FLEXIBLE PAVEMENTS USING FINITE-LAYER MODELING

Julián Andrés Pulecio Díaz¹, Myriam Rocío Pallares M² and Wilson Rodríguez Calderón¹

¹Civil Engineering Program, Faculty of Civil Engineering, Universidad Cooperativa de Colombia, Colombia

²Civil Engineering Program, Faculty of Engineering, Universidad Surcolombiana, Colombia

E-Mail: myriam.pallares@usco.edu.co

ABSTRACT

The effect of a suspension system on the design parameters of asphalt layer in a flexible pavement using finite layers freeware "3D-Move Analysis V2.1" is evaluated. This is done trying to reproduce more closely the contact and stress of the design axle (80kN) having as new input variables the damping and dynamic movement which are not currently applied in Colombian practice. To validate, the elastic multilayer EverStress software was used. The results of the strain can conclude that the asphalt pavement designs developed with analytical methods may be slightly oversized and consequently, the cost of construction of pavements increases. This study allows to analyze the sensitivity of various factors that may affect the design of asphalt pavements.

Keywords: 3D-Move analysis V2.1, everstress, damping, dynamic movement, road roughness, DLC, freeware pavement modeling.

1. INTRODUCTION

Currently, in the design of pavement structures, analytical methods and/or numerical models are used, in which these variables must be defined: the design axle (single axle of 8.2T (80kN) with four wheels, two at each end), the thickness of the layers and the characteristics of the materials. Hence, tensile strain in the lower and upper fibers of the asphalt layers (fatigue) can be calculated, accumulated permanent vertical strain of the asphalt layers and vertical strain in the granular and subgrade layers (permanent strain), caused by the contact pressure of the design load that is usually homogeneously applied in a circular area on the road surface as illustrated in Figure-1. This variable has been a subject of research studies that state that "contact pressure is not distributed uniformly, which provides some information to justify why the assumption of conventional contact area is incorrect"[1]. This statement has provided the basis of a study to evaluate the effect of the vehicle suspension system on the design parameters of the asphalt layers of a flexible pavement (horizontal strain " ϵ_{xx} " and " ϵ_{yy} "). For this purpose, the finite layer modeler 3D-Move Analysis V2.1 was used, it allows to reproduce the intensity of effort generated by the tires of the design vehicles, and the elastic multilayer software EverStress© 5.0 was used to validate the results.

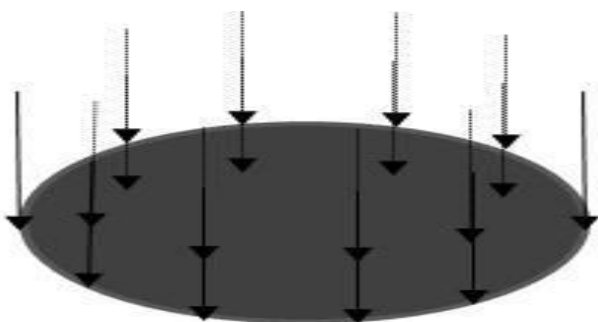


Figure-1. Circular contact area.

2. METHODS

The analysis was performed through the computational modelers, EverStress© 5.0 and 3D-Move Analysis V2.1; the first modeler was used to validate the results of finite layer modeling given its versatility and functionality. The asphaltic pavement structure represented is flexible and composed of a sub-base and granular base and a surface layer made of asphalt concrete as shown in Figure-2 [2] [3].

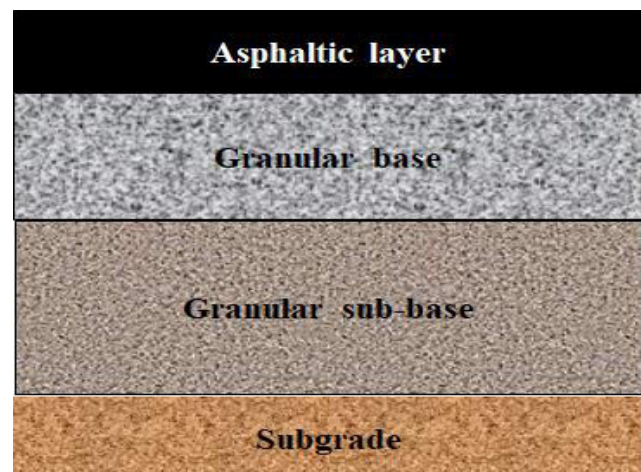


Figure-2. Flexible pavement structure modelling.

The dimensions of the modeled pavement structure layers are shown in Table-1. The boundary condition considered for the subgrade is semi-infinite and, as commonly used in the dimensioning of this type of structures, linked interfaces were used.



Table-1. Common values of layer thicknesses of a flexible pavement structure.

Layer	Thickness (m)	Thickness (in)
Asphalt surface	0,10	3,94
Granular base	0,20	7,87
Granular sub-base	0,30	11,81
Sub-grade	semi-infinite	semi-infinite

The elastic modulus taken as a reference for each of the layers according to the working conditions of the pavement are shown in Table-2. The elastic modulus of the subgrade known as resilient is determined by triaxial tests; the elastic modulus of the asphalt layers is established through tests of resilient or dynamic modulus at design temperatures and frequencies [4] [5] [6] or through experimental sections on which deflectionometer tests are performed, such as Falling Weight Deflectometer (FWD) or Heavy Weight Deflectometer (HWD), associated to inverse or back-calculation analysis and corrected to laboratory conditions and temperature [7] [8] [9] [10].

Table-2. Common values of elastic modulus on layers.

Layer	Elastic Modulus (MPa)	Elastic Modulus (PSI)
Asphalt surface (25°C, 5Hz)	1500	217500
Granular base	328	47589
Granular sub-base	148	21489
Sub-grade	49	7105

Since the variation of the Poisson's ratio has no significant impact on pavement behavior [2] [3], the characteristic values shown in Table-3 were used. The common thicknesses, the elastic modulus and the Poisson's ratio were taken from the study entitled "Three-dimensional modeling of pavement with dual load using finite element" [3].

Table-3. Common values of Poisson's ratio in the constitutive layers.

Layer	Poisson's Ratio
Asphalt surface	0,40
Granular base	0,40
Granular sub-base	0,45
Sub-grade	0,49

The determination of pavement design parameters have basis in the mechanical-empirical design that consists of modeling the structure based on the definition of thicknesses and stiffnesses, (resilient and

dynamic modulus, and the Poisson's ratio) of each layer in order to calculate the tensile and compression forces caused by a type load and to identify: a) strain at maximum tensile force (ϵ_t) capable of causing rupture of asphalt layers (fatigue) [11]; this strain is compared with the allowable limit of the asphalt material (ϵ_{tadm}) which is a function of multiple factors, including transit, thickness, elastic modulus with frequency and temperature, volumetric properties of the asphalt mix, regression coefficients, and origin and direction of the cracking [5]; b) the accumulated permanent vertical strain (ϵ_p) capable of producing rutting in the asphalt layers; this strain is compared with the allowable limit of the asphalt material (ϵ_{padm}) which is a function of multiple factors, including traffic, layer temperature, resilient vertical strain imposed in the laboratory test to obtain the properties of the material, depth confinement factor, depth below the surface and regression coefficients [5]; c) the maximum compression strain (ϵ_c) on the granular and subgrade layers, which is compared to the allowable compression strain (ϵ_{cadm}) and it depends on the transit, resilient vertical strain imposed in the laboratory test to obtain the properties of the material, thickness, etc.[5].

2.1 Analytical modeling EverStress© 5.0

The model was developed in the multi-layer elastic stress and strain calculation program for pavement design, EverStress© 5.0 [12], introducing a uniformly distributed inflation pressure over a circular radius area of 0,108m with a pressure of 0,560 MPa and a wheelbase of 0, 324 m.

The analysis allows to identify the characteristic strains of the pavement structural design control, such as tensile and compression strains in the asphalt layers and compression at the top of the granular and subgrade layers [5]. The location of these parameters is shown in Figure-3.

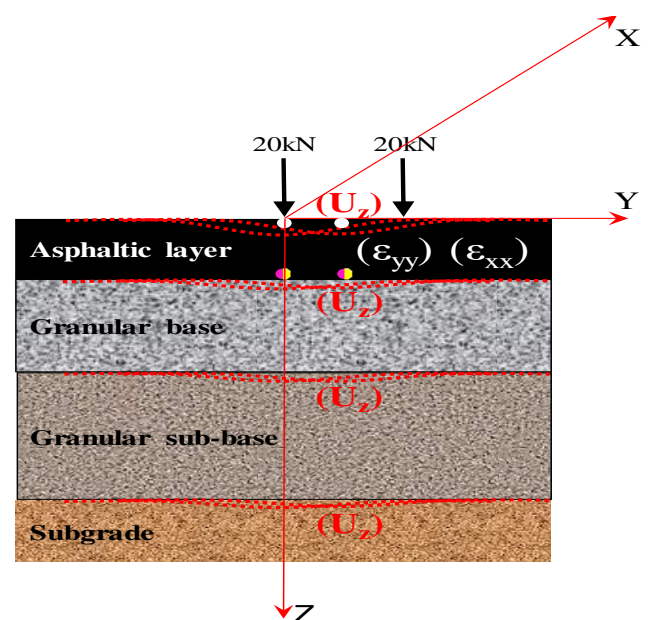


Figure-3. Location of the control parameters in the pavement design using EverStress© 5.0.



2.2 Finite layer modeling with 3D-Move Analysis V2.1

Finite layer modeling with 3D-Move Analysis V2.1 were validated using EverStress© 5.0. The 3D-Move Analysis V2.1 program works with meshes of different types of refinement in the cross section of the pavement and longitudinally with Fourier series. It consists of six interfaces (see Figure-4) that perform different functions: a) Project, location and identification, type of modeling (static or dynamic response) and possibility of performance analysis b) Inputs, axle configuration / contact pressure distribution, vehicle suspension / road roughness, traffic information, structure type and pavement layer properties c) Performance models, extended pavement analysis, d) Response points, location of stress-strain pavement responses, e) Output, responses required, stresses and main strains, and displacements, f) Results, allows to obtain the analysis results. Common steps of the analysis procedure of a stress-strain problem using 3D-Move Analysis V2.1, are: input project location, type of model (static or dynamic), with or without performance evaluation, axle configuration and contact pressure distribution, type of vehicle suspension and road roughness, sizing data, number of layers, thicknesses and stiffness parameters (resilient and dynamic modulus, and Poisson's ratio), location of required answers, run the solver and obtain results [13].

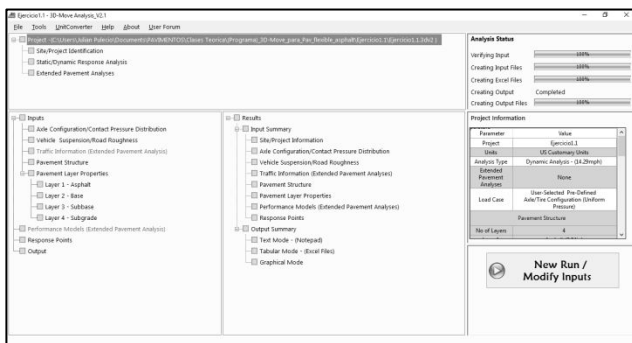


Figure-4. Interface of 3D-Move Analysis V2.1.

2.2.1 Vehicle suspension, road roughness and vehicle speed

Once the finite layer modeling was validated with the circular contact area and static condition, additional modeling was developed by changing the condition from a static modeling to a dynamic modeling (necessary in order to activate the effect of the vehicle suspension system), adding type of suspension system (see Figure-5) and road roughness, which are governed by the Dynamic Load Coefficient (DLC) parameter, a simple measurement of the magnitude of the dynamic change of the load axle for a specified combination of roughness, road speed and suspension system [14]. The purpose of the DLC is to measure the load perturbation, which is calculated from equation (1) and is shown in the Figure-6.

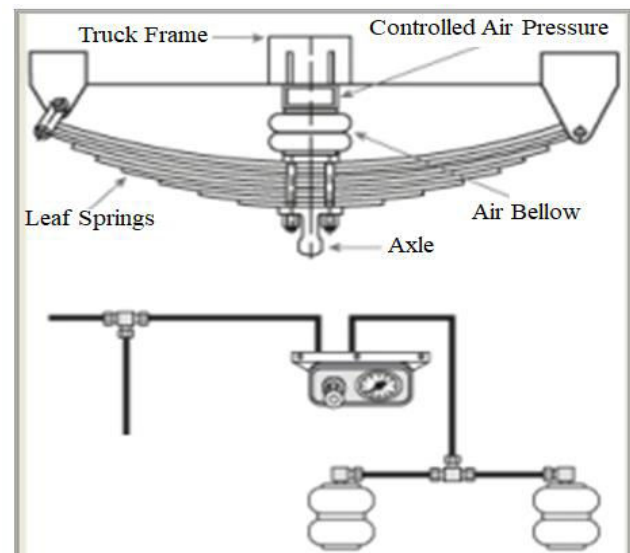


Figure-5. Vehicle suspension type four spring (Leaf Spring). Source: [13].

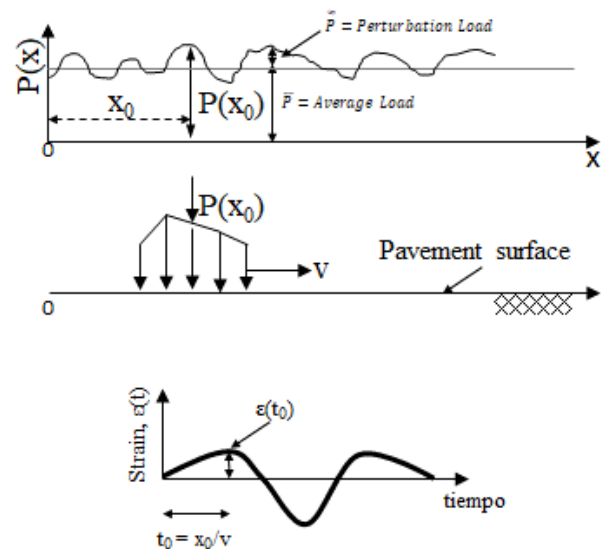


Figure-6. Load perturbation depending on vehicle speed, type of suspension and road roughness [13].

$$DLC = \frac{\tilde{P}(x)}{\bar{P}} \quad (1)$$

In order to correlate the roughness of the road with the vehicle's damping and speed system, the research project entitled "Effects of heavy vehicle characteristics on pavement response and performance" was used, which synthesizes that suspension systems type "4-Spring Flat-Leaf", the behavior of speed, DLC and roughness, behave as shown in Figure-7. The roughness is correlated to the International Roughness Index (IRI), common field measurement variable that indicates the level of service provided by the road to the user and allows monitoring the progress in the deterioration or recovery experienced by the road network [14].

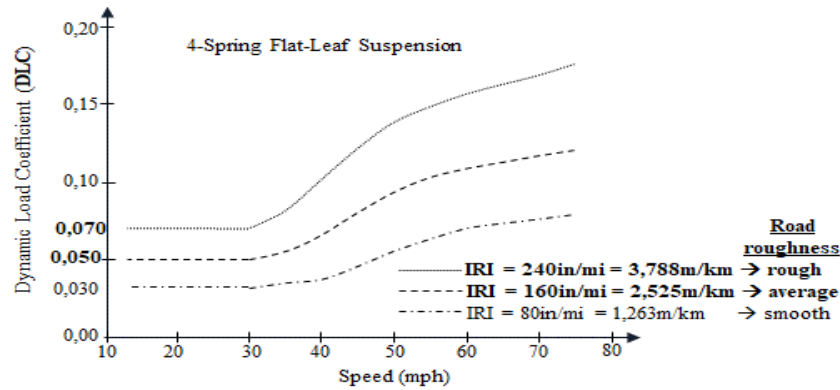


Figure-7. Vehicle behavior with suspension system “4-Spring Flat-Leaf”, speed, DLC and roughness. Source: [14].

In order to establish a case analysis, the conditions of interurban motorways in Colombia are chosen, which based on experience, have been determined

to be in a good condition ($2 < IRI \leq 3,5$ m/km) to fair ($3,5 < IRI \leq 5$ m/km) and in terms of roughness, it is average to rough, as shown in Table-4.

Table-4. IRI values, classification, PSI and common road roughness on interurban motorways.

IRI (in/mi) *	IRI (m/km)	Classification	PSI ^{1,2}	Road roughness ³
240	3,788	Fair	2,5	Rough
160	2,525	Good	3,4	Average
80	1,263	Excellent	4,25	Smooth
0	0	-	5	-

^{1,3} Taken from [14]

²Present Serviceability Index (PSI) of a pavement

Lastly, the vehicle speed (s) was obtained using equation (2) shown in the book “Pavement analysis and design” [15], which is a function of the tire contact radius (a) (Figure-8) duration of load (t) (Figure-9). The duration of the load (t), is obtained using the inverse of the test frequency (1/f) in the resilient modulus of the asphalt layer and the tire contact radius (a), which is established for a design axle of 8,2T (80kN) in Colombia.

$$s = \frac{12a}{t} = \frac{12 \times 10,8 \text{ cm}}{0,20 \text{ seg}} = 648 \text{ cm/s} \approx 23 \text{ kph} \approx 14,29 \text{ mph}$$

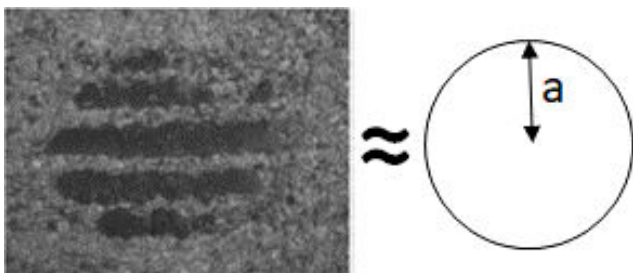


Figure-8. Tire contact radius (a). Source:[16].

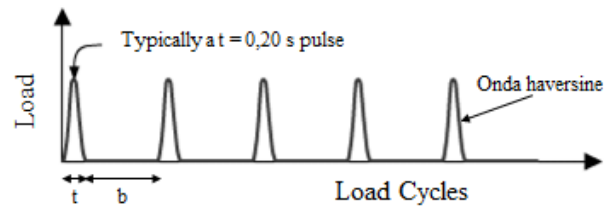


Figure-9. Duration of load (t) in a resilient modulus test.

2.3. AASHTO-MEPDG 2015 transfer functions

Transfer functions were applied from AASHTO-MEPDG 2015, calculating the accumulative equivalent single axles loads of 80 kN in the design lane (ESAL’s) using equations (3), (4), (5) and (6).

$$N_f = 0,00432 * 0,007566 * k_1 * C * \left(\frac{1}{e_t}\right)^{3,9492} * \left(\frac{1}{E}\right)^{1,281} \quad (3)$$

$$C = 10^M \quad (4)$$

$$M = 4,84 \left(\frac{V_b}{V_a + V_b} - 0,6875 \right) \quad (5)$$

$$k_1 = \frac{1}{0,000398 + \left(\frac{0,003602}{1 + e^{(11,02 - 3,49 * hac)}} \right)} \quad (6)$$



Where N_f is the allowable number of load repetitions to prevent fatigue cracking, which is equal to the ESAL's, ϵ_t is the maximum tensile strain capable of producing fatigue cracking on the asphalt layers, E is the elastic modulus with frequency and temperature units of lb/in^2 , V_b is the volume percentage of the bitumen in %, V_a is the percentage volume of void in %, k_1 is the adjustment factor for different effects of the asphalt layer thickness, such as cracking in the top of the layer and in the asphalt layer thickness, in inches.

3. RESULTS AND DISCUSSIONS

The results of the analytical model performed using EverStress© 5.0 (used as a validation method) and the finite layer modeling using 3D-Move Analysis V2.1

are shown in Table-5. It is important to note that the sign convention of EverStress© 5.0 is positive (+) for tension and negative (-) for compression, as opposed to the sign convention of 3D-Move Analysis V2.1, which is positive (+) for compression and negative (-) for tension; henceforth, the results of the strain will be displayed as (T) for tension, and (C) for compression.

As shown in Table-5, the change percentage of the numerical model compared to the analytical model are lower than 1.10%, which allows to conclude that the decisions made in the modeling with 3D-Move Analysis V2.1 are suitable to implement in the models that introduce modifications such as type analysis from static to dynamic, activation of the vehicle suspension system and road roughness.

Table-5. Validation of design control results of the flexible asphalt pavement structure.

Layer	Location	Parameter	Analytical (EverStress© 5.0)	Numerical (3D-Move Analysis V2.1)	Variation
Asphalt surface	Under a tire	$\epsilon_{yy} \rightarrow \epsilon_t$	(T) 1,969E-04	(T) 1,972E-04	0,16%
Asphalt surface	Under a tire	$\epsilon_{xx} \rightarrow \epsilon_t$	(T) 2,738E-04	(T) 2,729E-04	0,32%
Asphalt surface	Under the center of the dual load	$\epsilon_{yy} \rightarrow \epsilon_t$	(C) 1,109E-04	(C) 1,097E-04	1,08%
Asphalt surface	Under the center of the dual load	$\epsilon_{xx} \rightarrow \epsilon_t$	(T) 2,348E-04	(T) 2,343E-04	0,20%

Figures 10 and 11 show the results of the analytical model and Figure-12 shows the results of modeling with 3D-Move Analysis V2.1; the underlined values are the design control parameters for fatigue in the asphalt layer, the superior fibers analysis is skipped due to its slimmess (thickness < 0,125 m) [17].

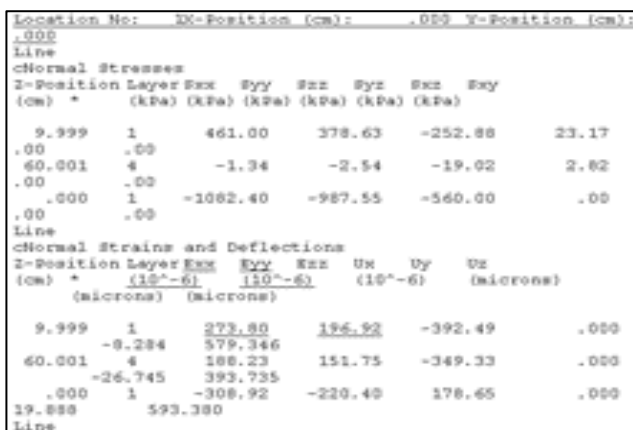


Figure-10. Results of the ϵ_{yy} and ϵ_{xx} strain in the lower fibers of the asphalt layer using EverStress © 5.0 under a wheel.

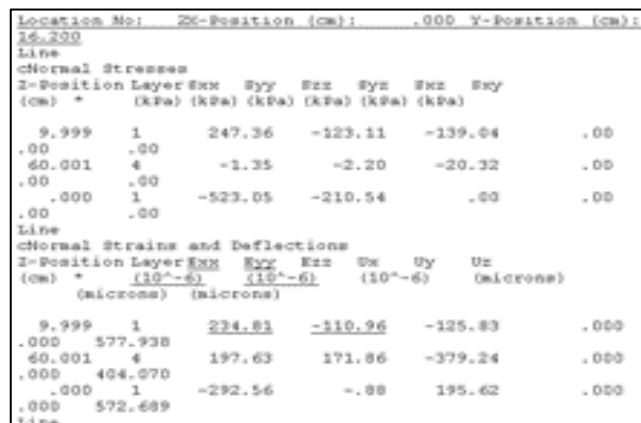


Figure-11. Results of the ϵ_{yy} and ϵ_{xx} strain in the lower fibers of the asphalt layer using EverStress © 5.0 under the center of the dual load.

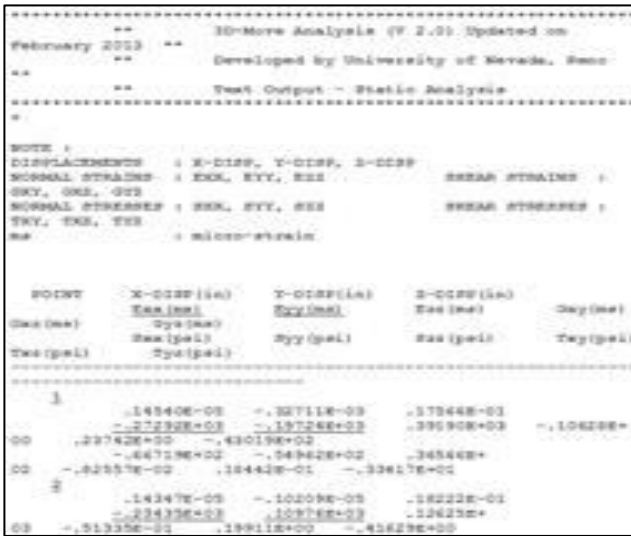


Figure-12. Results of the ϵ_{yy} and ϵ_{xx} strain in the lower fibers of the asphalt layer using 3D-Move Analysis V2.1 under the wheel and under the center of the dual load.

The results obtained shown in Figures 10, 11 and 12 verify that the maximum strain in the lower fibers of the asphalt layer are under the wheel and not under the center of the dual load.

3.1 Finite layer modeling with suspension system and road roughness

Two modeling were developed to analyze the response to strain of the asphalt pavement layer, with the new input variables: the damping and dynamic movement. The damping system is shown in Figure-5, the roughness is average to rough (Table-4), the vehicle speed (s) is calculated from equation (2) and the Dynamic Load Coefficient (DLC) is estimated from the type of damping, roughness and speed, which are 0,050 (average roughness) and 0,070 (rough)

3.1.1 Roads with average roughness - DLC equal to 0,050

Figure-13 shows the development of strain ϵ_{yy} in the lower fiber of the asphalt layer with DLC equal to 0,050 during a period of time from 0 to 10 seconds. Under the wheel at 4,87E-001 seconds, the maximum normal strain is found, $\epsilon_{yy} = (T) 1,574E-04$ ((T) 1,574E+002 micro strain). Henceforth, the result analysis will be developed according to the reference modeling with the elastic multi-layer software, for the calculation of stress and strain for pavement design in EverStress© 5.0 with constant pressure and circular contact area. When comparing the result of the maximum normal strain ϵ_{yy} with the reference modeling, it is found that the first one is smaller.

Figure-14 shows the development of strain ϵ_{xx} in the lower fiber of the asphalt layer with DLC equal to 0,050 during a period of time from 0 to 10 seconds. Under the wheel at 4,87E-001 seconds, the maximum normal strain is found, $\epsilon_{xx} = (T) 2,194E-04$ ((T) 2,194E+002 micro strain). When comparing the result of the maximum

normal strain ϵ_{xx} with the reference modeling, it is found that the first one is smaller.

Figure-15 shows the development of strain ϵ_{yy} in the lower fiber of the asphalt layer with DLC equal to 0,050 during a period of time from 0 to 10 seconds. Under the center of the dual load at 4,87E-001 seconds, the maximum normal strain is found, $\epsilon_{yy} = (T) 1,769E-04$ ((T) 1,769E+002 micro strain). When comparing the result of the maximum normal strain ϵ_{yy} with the reference modeling, it is found that it has an opposite behavior, since it has tension instead of compression.

Figure-16 shows the development of strain ϵ_{xx} in the lower fiber of the asphalt layer with DLC equal to 0,050 during a period of time from 0 to 10 seconds. Under the center of the dual load at 4,87E-001 seconds, the maximum normal strain is found, $\epsilon_{xx} = (T) 2,260E-04$ ((T) 2,260E+002 micro strain). When comparing the result of the maximum normal strain ϵ_{xx} with the reference modeling, it is found that the first one is smaller.

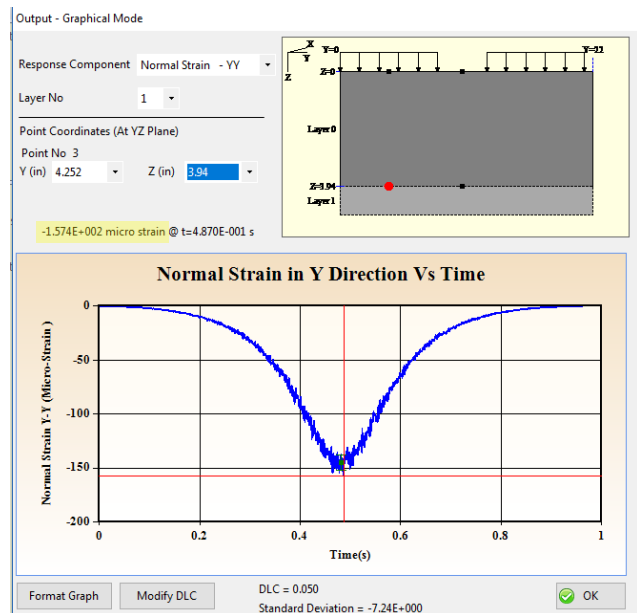


Figure-13. Strain ϵ_{yy} in the lower fiber of the asphalt layer under the wheel, using 3D-Move Analysis V2.1.

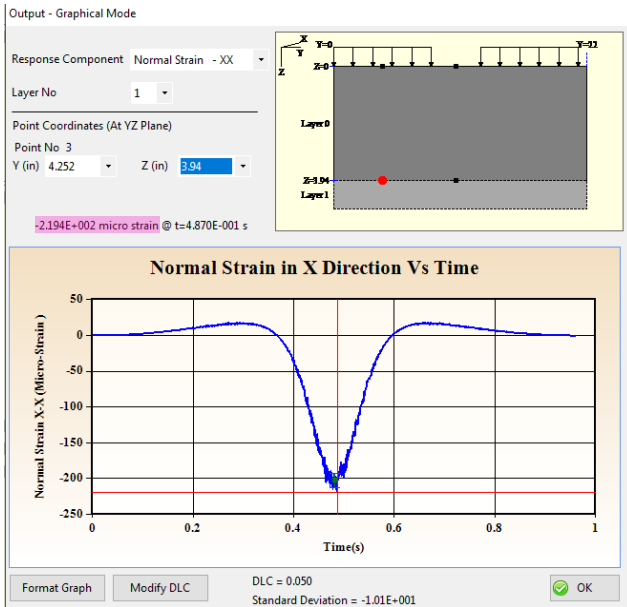


Figure-14. Strain ϵ_{xx} in the lower fiber of the asphalt layer under the wheel, using 3D-Move Analysis V2.1.

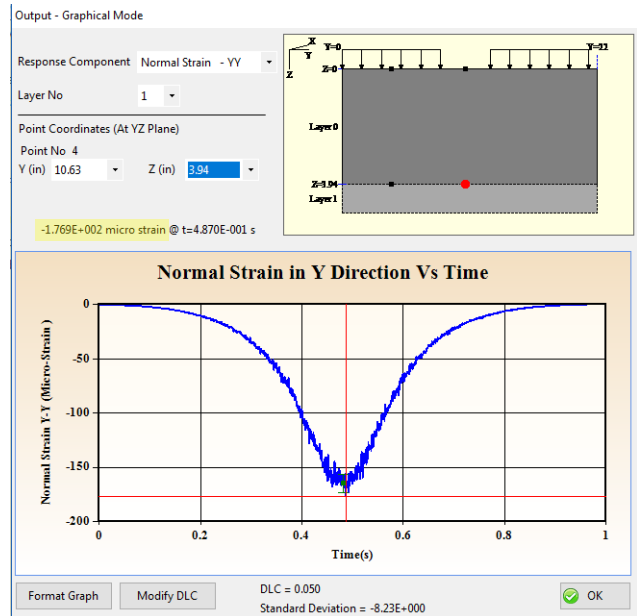


Figure-15. Strain ϵ_{yy} in the lower fiber of the asphalt layer under the center of the dual load, using 3D-Move.

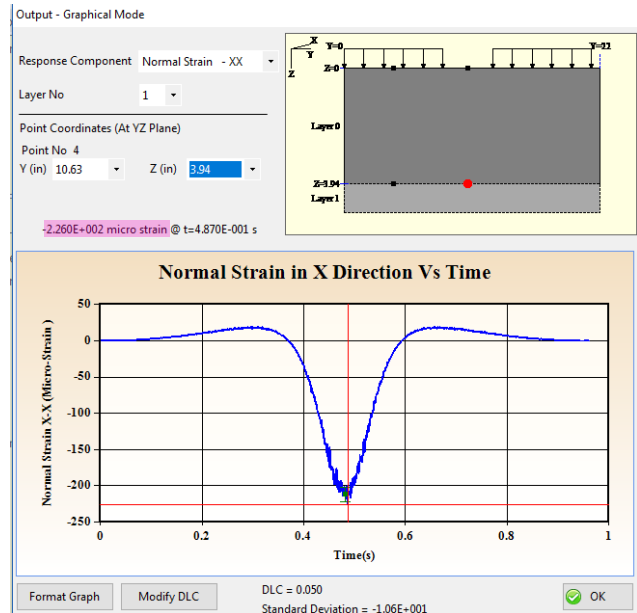


Figure-16. Strain ϵ_{xx} in the lower fiber of the asphalt layer under the center of the dual load, using 3D-Move.

Table-6. Variation of the structural design control parameters of a flexible pavement with DLC equal to 0,050.

Layer	Location	Parameter	Analytical (EverStress© 5.0)	Numerical (3D-Move Analysis V2.1)	Variation
Asphalt surface	Under a tire	$\epsilon_{yy} \rightarrow \epsilon_t$	(T) 1,969E-04	(T) 1,574E-04	20,07%
Asphalt surface	Under a tire	$\epsilon_{xx} \rightarrow \epsilon_t$	(T) 2,738E-04	(T) 2,194E-04	19,87%
Asphalt surface	Under the center of the dual load	$\epsilon_{yy} \rightarrow \epsilon_t$	(C) 1,109E-04	(T) 1,769E-04	-
Asphalt surface	Under the center of the dual load	$\epsilon_{xx} \rightarrow \epsilon_t$	(T) 2,348E-04	(T) 2,260E-04	3,75%



Table-6 includes the result summary compared with the obtained in the elastic multilayer modeling using EverStress 5.0, determining a significant change percentage.

3.1.2 Roads with rough roughness - DLC equal to 0,070

Figure-17 shows the development of strain ϵ_{yy} in the lower fiber of the asphalt layer with DLC equal to 0,070 during a period of time from 0 to 10 seconds. Under the wheel at 4,87E-001 seconds, the maximum normal strain is found, $\epsilon_{yy} = (T) 1,618E-04$ ((T) 1,618E+002 micro strain). When comparing the result of the maximum normal strain ϵ_{yy} with the reference modeling, it is found that the first one is smaller.

Figure-18 shows the development of strain ϵ_{xx} in the lower fiber of the asphalt layer with DLC equal to 0,070 during a period of time from 0 to 10 seconds. Under the wheel at 4,87E-001 seconds, the maximum normal strain is found, $\epsilon_{xx} = (T) 2,260E-04$ ((T) 2,260E+002 micro strain). When comparing the result of the maximum normal strain ϵ_{xx} with the reference modeling, it is found that the first one is smaller.

Figure-19 shows the development of strain ϵ_{yy} in the lower fiber of the asphalt layer with DLC equal to 0,070 during a period of time from 0 to 10 seconds. Under the center of the dual load at 4,87E-001 seconds, the maximum normal strain is found, $\epsilon_{yy} = (T) 1,813E-04$ ((T) 1,813E+002 micro strain). When comparing the result of the maximum normal strain ϵ_{yy} with the reference modeling, it is found that it has an opposite behavior, since it has tension instead of compression. The result is similar to the result found in the road with average roughness. This statement led to recommend being careful with the analytical modeling results that do not have damping and dynamic movement of the design axle. Notice that, if normal tensile strains in the lower fibers of the asphalt layers exist, it is a control factor in the design of asphalt pavements.

Figure-20 shows the development of strain ϵ_{xx} in the lower fiber of the asphalt layer with DLC equal to 0,070 during a period of time from 0 to 10 seconds. Under the center of the dual load at 4,87E-001 seconds, the maximum normal strain is found, $\epsilon_{xx} = (T) 2,313E-04$ ((T) 2,313E+002 micro strain). When comparing the result of the maximum normal strain ϵ_{xx} with the reference modeling, it is found that the first one is smaller.

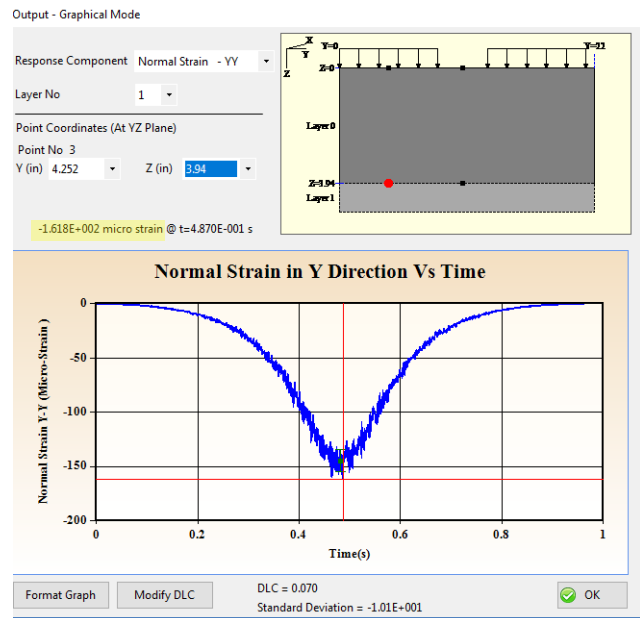


Figure-17. Strain ϵ_{yy} in the lower fiber of the asphalt layer under the wheel, using 3D-Move Analysis V2.1.

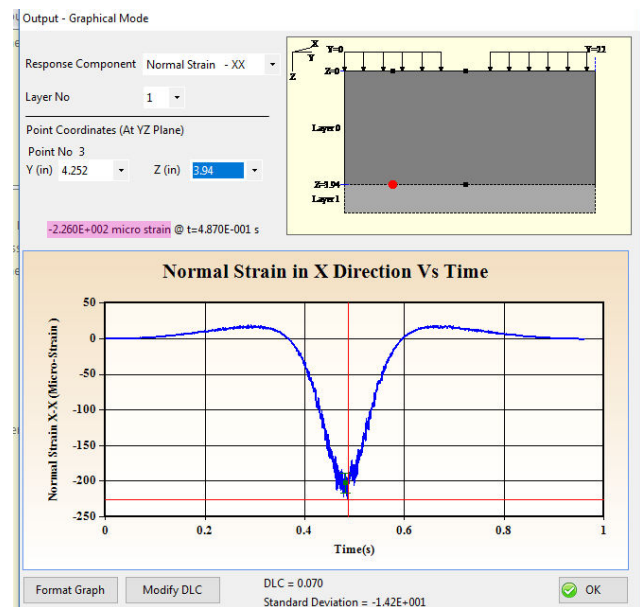


Figure-18. Strain ϵ_{xx} in the lower fiber of the asphalt layer under the wheel, using 3D-Move Analysis V2.1.

Table-7. Variation of the structural design control parameters of a flexible pavement with DLC equal to 0,070.

Layer	Location	Parameter	Analytical (EverStress© 5.0)	Numerical (3D-Move Analysis V2.1)	Variation
Asphalt surface	Under a tire	$\epsilon_{yy} \rightarrow \epsilon_t$	(T) 1,969E-04	(T) 1,618E-04	17,83%
Asphalt surface	Under a tire	$\epsilon_{xx} \rightarrow \epsilon_t$	(T) 2,738E-04	(T) 2,260E-04	17,46%
Asphalt surface	Under the center of the dual load	$\epsilon_{yy} \rightarrow \epsilon_t$	(C) 1,109E-04	(T) 1,813E-04	-
Asphalt surface	Under the center of the dual load	$\epsilon_{xx} \rightarrow \epsilon_t$	(T) 2,348E-04	(T) 2,313E-04	1,49%

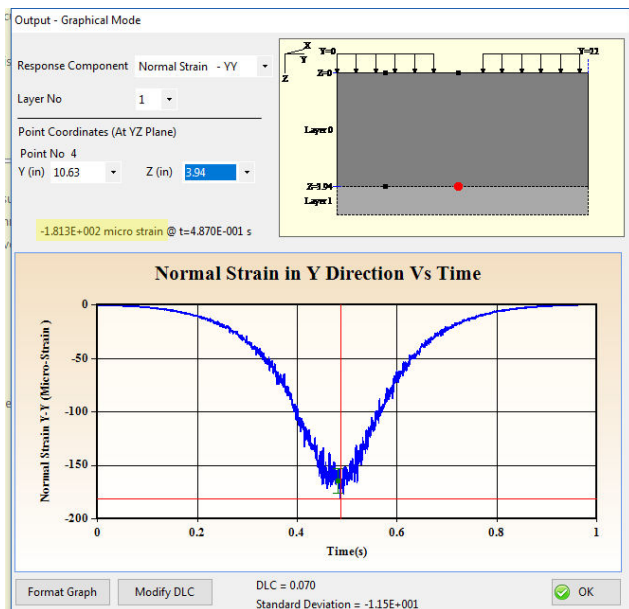


Figure-19. Strain ϵ_{yy} in the lower fiber of the asphalt layer under the center of the dual load, using 3D-Move Analysis V2.1.

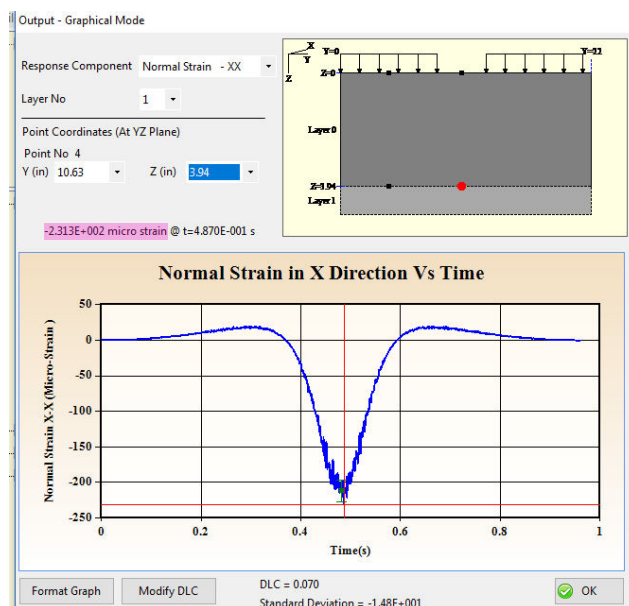


Figure-20. Strain ϵ_{xx} in the lower fiber of the asphalt layer under the center of the dual load, using 3D-Move Analysis V2.1.

Table-7 includes the result summary compared with the obtained in the elastic multilayer modeling using EverStress 5.0, determining a significant change percentage.

Therefore, it is found that values below those estimated with the reference model, led to conclude that the asphalt layer of flexible pavements is currently oversized. This is the particular case of flexible structures with low volume presented in the 1994 version of the French design manual for pavement structures [6], which does not consider stress-strain analysis in the asphalt layer,

requiring only a functional thickness of asphalt concrete or instead, a surface treatment.

4. CONCLUSIONS

- The results, obtained from the finite layer modeling developed with the free software 3D-Move Analysis V2.1, were successfully validated with the elastic multilayer analytical modeling, which allows to analyze the effect of the vehicle suspension system on the design parameters of flexible pavements.
- Free-use finite layer modelers such as 3D-Move Analysis V2.1 prove to be very useful and versatile tools, and they are great support for analysis such as the described, and it is adequate against commercial tools with a high cost and high learning and training curves.
- If the change percentage reported in the tables are carefully observed it is possible to conclude that the designs developed with analytical methods with fatigue control (upward cracking) are being slightly oversized. For example, the strain ϵ_{xx} obtained using the analysis of Everstress 5.0 and 3D-move with DLC = 0,050 (average) are: 2,738E-04 and 2,194E-04 respectively, which in terms of equivalent single axles with dual load of 80kN (8,2T), it is 296079 and 671029 ESAL's, with thicknesses of 0,10 m and 0,1457 m, showing a thickness difference of 0,0457 m (4,57cm), which in construction equals to an extra of 4 cm of thickness in the design, and consequently the construction costs increase.
- If the change percentage reported in the tables are carefully observed, it is possible to conclude that the designs developed with analytical methods with fatigue control (upward cracking) are being slightly oversized. For example, the strain ϵ_{xx} obtained using the analysis of Everstress 5.0 and 3D-move with DLC =0,070 (rough) are: 2,738E-04 and 2,260E-04 respectively, which in terms of equivalent single axles with dual load of 80kN (8,2T), it is 296079 and 596986 ESAL's, with thicknesses of 0,10 m and 0,1401 m, which in construction equals to an extra of 4 cm of thickness in the design, and consequently the construction costs increase.
- In general terms, if quality is fulfilled in the construction, such as evaluating each layer of the pavement through on-site performance evaluation equipment, in addition, respecting routine maintenance protocols and other works that guarantee local and global stability (drainage) and global stability of the area, in construction, the thickness of the asphalt layer could be reduced by 4 cm, generating savings between \$ 53,200,000 to \$ 57,400,000 Colombian pesos, in the case of a kilometer of pavement with lane width of 3.50 m and dense mix in a conventional heat.
- The finite layer method has proven to be very effective and in a particular case, it allowed to evaluate the effect of the vehicle suspension system on the flexible pavement design parameters, therefore, it establishes a way to study the sensitivity of different



factors that can affect the design of asphalt pavements.

- The interest of learning more about the effect of the vehicle suspension system on the flexible pavement design parameters has developed, in future studies, dynamic conditions will most likely be analyzed introducing results obtained from real-scale tests.

REFERENCES

- [1] K. Xia. 2010. Finite Element Modeling of Dynamic Tire/Pavement Interaction. Pavements and Materials: Testing and Modeling in Multiple Length Scales. pp. 204-214.
- [2] W. Rodríguez-Calderón y M. R. Pallares-Muñoz. 2005. Desarrollo de un modelo de elementos finitos para el diseño racional de pavimentos. *Tecnura*. 9(17): 25-37.
- [3] W. Rodríguez-Calderón y M. R. Pallares-Muñoz. 2015. Three-dimensional modeling of pavement with degree load using finite element. *DYNA*. 82(189): 30-38.
- [4] N. Kringos, B. Birgisson, D. Frost y L. Wang. 2013. Multi-Scale Modeling and Characterization of Infrastructure Materials, Switzerland: Springer Netherlands.
- [5] AASHTO. 2015. Mechanistic-empirical pavement design guide, A Manual of Practice, United States of American: American Association of State Highway and Transportation Officials.
- [6] LCPC. 1994. Conception et dimensionnement des structures de chaussée, Guide technique, Paris, France: LCPC and SETRA.
- [7] C. Rabaiotti, A. Puzrin, M. Caprez y C. Ozan. 2013. Pavement structural health evaluation based on inverse analysis of three dimensional deflection bowls. *International Journal of Pavement Engineering*. 14(4): 374-387.
- [8] A. Papagiannakis y E. Masad. 2008. Pavement design and materials. United States of American: John Wiley & Sons.
- [9] G. Beltran y M. Romo. 2014. Assessing artificial neural network performance in estimating the layer properties of pavements. *Ingenieria e Investigación*. 34(2): 11-16.
- [10] R. Mallick y El-Korchi. 2018. Pavement engineering: principles and practice, United States of American: CRC Press Taylor & Francis Group.
- [11] J. Tamayo. 1985. Comportamiento de los materiales bajo carga repetida. *Ingeniería e Investigación*. (12): 22-29.
- [12] 1999. Washington State Department of Transportation, Theory Manual, Washington: Washington State Department of Transportation.
- [13] University of Nevada. 2013. Theory Manual, 3D-Move Analysis Software, Reno, United States of American: Asphalt Research Consortium, University of Nevada.
- [14] T. Gillespie. 1993. Effects of Heavy-vehicle Characteristics on Pavement Response and Performance. Transportation Research Board. p. 136.
- [15] Y. Huang. 2004. Pavement analysis and design. Kentucky United States of American: Prentice hall.
- [16] A. Das. 2015. Analysis of pavement structures. United States of American: CRC Press Taylor & Francis Group.
- [17] Kallas y Puzinauskas. 1972. Flexural Fatigue Tests on Asphalt Paving Mixtures. American Society of Testing and Materials (ASTM).